AD-A123 301 CERAMIC LIFE PREDICTION METHODOLOGY - ANALYTICAL ASSESSMENT OF SELECTED COMPONENT DATA(U) FORD MOTOR CO DEARBORN MICH L R SWANK SEP 82 AMMRC-TR-82-50 1/1

UNCLASSIFIED DAAG46-77-C-0028 F/G 11/2 NL

END

FILMED

DTIC

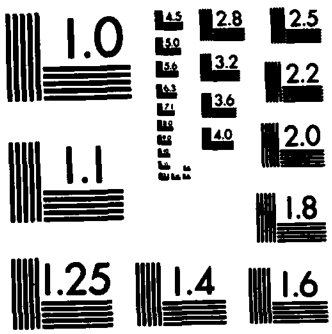
1.0
2.8
2.5
3.2
2.2
3.6
4.0
2.0
1.1
1.8
1.25
1.4
1.6

6

ADA123301

AD

AMMRC TR 82-50

CERAMIC LIFE PREDICTION METHODOLOGY - ANALYTICAL ASSESSMENT OF SELECTED COMPONENT DATA

September 1982

L. R. SWANK
Ford Motor Company
Dearborn, Michigan 48121

INTERIM REPORT

Contract No. DAAG46-77-C-0028

Approved for public release; distribution unlimited.

Prepared for

ARMY MATERIALS AND MECHANICS RESEARCH CENTER
Watertown, Massachusetts 02172

UNCLASSIFIED

SECURITY CLASSIFICATION OF THIS PAGE (When Data Entered)

REPORT DOCUMENTATION PAGE		READ INSTRUCTIONS BEFORE COMPLETING FORM
1. REPORT NUMBER AMMRC TR 82-50	2. GOVT ACCESSION NO. AD-A123 302	3. RECIPIENT'S CATALOG NUMBER
4. TITLE (and Subtitle) CERAMIC LIFE PREDICTION METHODOLOGY - ANALYTICAL ASSESSMENT OF SELECTED COMPONENT DATA		5. TYPE OF REPORT & PERIOD COVERED Interim - July 81 to Feb 82
		6. PERFORMING ORG. REPORT NUMBER
7. AUTHOR(s) L. R. Swank		8. CONTRACT OR GRANT NUMBER(s) DAAG46-77-C-0028
9. PERFORMING ORGANIZATION NAME AND ADDRESS Ford Motor Company Dearborn, Michigan 48121		10. PROGRAM ELEMENT, PROJECT, TASK AREA & WORK UNIT NUMBERS
11. CONTROLLING OFFICE NAME AND ADDRESS Army Materials and Mechanics Research Center ATTN: DRXMR-K Watertown, Massachusetts 02172		12. REPORT DATE September 1982
		13. NUMBER OF PAGES 24
14. MONITORING AGENCY NAME & ADDRESS(if different from Controlling Office)		15. SECURITY CLASS. (of this report) Unclassified
		15a. DECLASSIFICATION/DOWNGRADING SCHEDULE

16. DISTRIBUTION STATEMENT (of this Report)

Approved for public release; distribution unlimited.

17. DISTRIBUTION STATEMENT (of the abstract entered in Block 20, if different from Report)

18. SUPPLEMENTARY NOTES

19. KEY WORDS (Continue on reverse side if necessary and identify by block number)

Ceramic materials	Life expectancy	Mechanical properties
Silicon nitrides	Finite element analysis	
Gas turbine rotors	High temperature	

20. ABSTRACT (Continue on reverse side if necessary and identify by block number)

(SEE REVERSE SIDE)

DD FORM 1 JAN 73 1473 EDITION OF 1 NOV 65 IS OBSOLETE

UNCLASSIFIED

SECURITY CLASSIFICATION OF THIS PAGE (When Data Entered)

Block No. 20

ABSTRACT

A complete set of thermal conditions, mechanical loads, geometry as well as thermal, elastic, fast fracture, and time dependent material properties was furnished by AMMRC for the hub of a gas turbine disc. A finite element computer model was prepared for the disc from this data. The temperture and stress distributions, the fast fracture and the time dependent reliabilities were calculated. The results were presented in iso-stress and iso-thermal plots and in graphical data.

Foreword

This report represents the analysis of a structural ceramic component selected by AMMRC. The component selected was the hub of a hot pressed silicon nitride turbine rotor. The required geometrical, material, strength, and time dependent data was supplied by AMMRC. This work was conducted as part of the "Methodology for Ceramic Life Program," initiated by Dr. Robert Schulz of the Office of Conservation, division of Transportation Systems, Department of Energy, and monitored by the Army Materials and Mechanics Research Center under Contract Number DAAG-46-77-C-0028. This work was part of the continuing investigation of analytical and experimental methods in ceramic life prediction aimed toward utilizing structural ceramics in high temperature applications. The principal investigator of this program was R. R. Baker, Ceramic Materials Department, engineering and Research Staff, Ford Motor Company. The technical monitor was Dr. E. M. Lenoe of AMMRC. The author wishes to thank Drs. E. M. Lenoe and R. N. Katz of AMMRC for suggestions in carrying out the program.

TABLE OF CONTENTS

1. INTRODUCTION

This report presents the analysis of a gas turbine disc based on data supplied by AMMRC. The data supplied was the disc's geometry, its rotational speed, forces to simulate the blade loads, heat transfer coefficients and corresponding fluid temperature. Also supplied were the material's elastic, fast fracture, and time dependent properties.

The primary purpose of the analysis was to calculate reliability versus time for the steady state speed and temperature conditions. The time dependent theory used is explained in Section 2. In order to complete a time dependent reliability analysis it is necessary to calculate the reliability at time equals zero which is the fast fracture reliability. Weibull theory was used for calculation of fast fracture reliability and the theory is briefly reviewed in Section 3.

The stresses and temperatures were calculated with finite element computer programs and the results are plotted in contour plots. For reference the stresses due to mechanical loads at room temperature were calculated and plotted. The data supplied by AMMRC was reproduced here in the tabular form required by the computer codes used in the analysis.

2. TIME DEPENDENT THEORY

The prediction of time to failure in structural ceramics is usually based on the equation

$$V = AK_I^{\,n} \,. \qquad (1)$$

This equation relates the velocity of a crack in the material to the stress intensity factor of the tip of the crack. Siverns[1] observed this behavior in steel and published velocity versus stress intensity data and fitted the constant "A" and crack velocity exponent "n" to the data with linear regression analysis[2]. Evans[3] observed similar behavior in ceramic materials and using the fracture mechanics equation

$$K_I = \sigma Y a^{1/2} \qquad (2)$$

arrived at the following equation for calculating crack growth versus time[4].

$$\int_o^t AY^n \sigma^n dt = \frac{2}{(n-2)} \left[\left(\frac{1}{a_o}\right)^{\frac{n-2}{2}} - \left(\frac{1}{a}\right)^{\frac{n-2}{2}} \right] \qquad (3)$$

Equation 3 applies only to a single crack in a uniform stress field. To allow calculation of time dependent failure in complex structures, Paluszny[5] combined the ideas in Equation 3 with the Weibull[6] equation for calculating fast fracture reliability in brittle materials and arrived at Eqn. 4.

$$R = \exp\left[- \left[\left(\ln\left(\frac{1}{R_{ff}}\right)\right)^{\frac{n-2}{m}} + \frac{\sigma^n t}{\sigma_\theta^{n-2} B} \right]^{\frac{m}{n-2}} \right] \tag{4}$$

Equation 4 was reduced to Eqn. 5 in Reference 7.

$$R = R_{ff}^{\left(1+\frac{\sigma^n t}{B}\right)^{\frac{n-2}{m}}} \tag{5}$$

In this study Eqn. 5 was used to calculate the reliabilities versus time of complex structures by dividing the structure into small elements where the stress was considered constant and evaluating Eqn. 5, the reliability of a structure with "q" elements was then calculated with Eqn. 6.

$$R = R_1 \cdot R_2 \cdot R_3 \dots R_q \tag{6}$$

This technique is suitable for use with finite element stress programs where R_i is evaluated for each element. The constant in Eqn. 5 is given as Eqn. 7[5].

$$B = \frac{2}{(n-2)Y^2 A K_{IC}^{n-2}} \tag{7}$$

Equations 5, 6, and 7 were used in this report to calculate time dependent reliability.

3. WEIBULL THEORY

The evaluation of Eqn. 5 requires that the fast fracture reliability be evaluated. For this study, the Weibull[6] equation was used. Weibull proposed that each element of a structure has a definite probability of failure and that the entire structure could be considered to be an assembly of the individual elements and their associated probability of failure. Vardar and Finnie[8] give an integral formulation of the Weibull approach:

$$P_f = 1 \exp^{-B} = 1 - \exp\left[- \int_V \left(K \int_A \sigma_n^m \, dA\right) dV \right] \tag{8}$$

The term in the parentheses is evaluated on the surface of the unit sphere (Fig. 1), over the regions where the normal stress is tensile and neglecting regions where the normal stress is compressive. The reasons for neglecting compressive stress are 1) for structural ceramics, compression is not as detrimental in causing fracture as is tension, and 2) mathematical complexities are minimized[9]. The normal stress on the surface of the unit sphere in terms of the maximum principal stresses and the polar and azimuthal angles is given by:

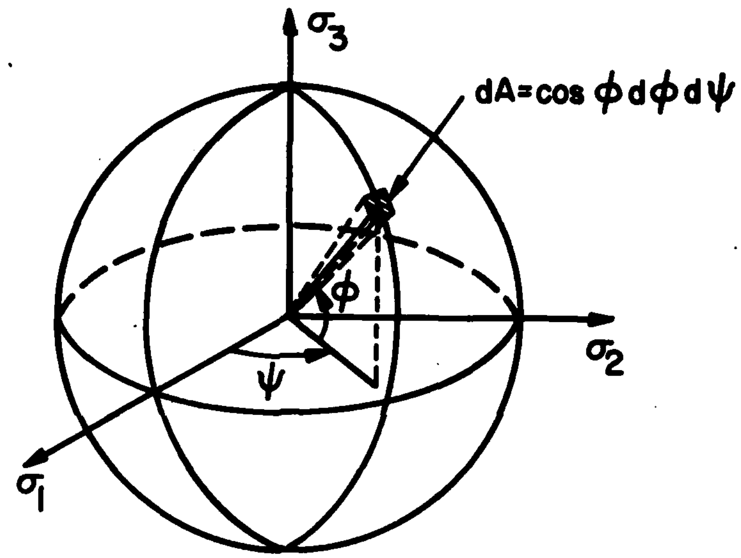

Fig. 1. Geometric variables describing location on unit sphere

$$\sigma_n = \cos^2\phi(\sigma_1\cos^2\psi + \sigma_2\sin^2\psi) + \sigma_3\sin^2\phi \qquad (9)$$

The constant, K, is given by:

$$K = \frac{2m + 1}{2\pi\sigma_o{}^m} \qquad (10)$$

The $(2m+1)/2\pi$ term in Eq. 10 is a compatability factor required to make the result of integrating Eq. 8 using the normal stress distribution of Eq. (9) for uniaxial stress cases, agree with the results obtained from the one-dimensional Weibull equation:

$$P_f = 1 - \exp \int_V (\frac{\sigma}{\sigma_o})^m \, dV \qquad (11)$$

The integration of Eq. 8 over an entire structure is accomplished by dividing the structure into finite elements in which the principal stresses can be assumed to be constant. The result of integrating over the unit sphere is constant in each finite element; therefore, the risk of rupture for each element is simply the volume of the element times the integrated result over the unit sphere. This procedure is very convenient when used with finite-element stress programs and is the one used to calculate the probability-of-failure distributions for the structures in the present paper.

In the Weibull formulation, σ_o and m are parameters which show the probability of having a certain strength in any finite element. The values of σ_o and m are obtained from experimental test results. Weibull showed that the characteristic strength, σ_o, is identical to the ultimate strength of the material in the classical theory as the Weibull modulus, m, increases indefinitely. This result provides a physical interpretation of the characteristic strength. The Weibull modulus may be interpreted as a measure of variability in the strength distribution; as m increases, the variability of the strength diminishes.

For this report value of σ_o was calculated with Eqn. 12[10].

$$\sigma_o = MOR_o \left(\frac{bh}{2}\right)^{1/m} \left[\frac{L_1+mL_2}{(m+1)^2}\right]^{1/m} \qquad (12)$$

The parameters σ_o and m define the strength of the material and are independent of the volume and geometry of the structure. They are the values used to determine the failure distribution of a complex structure and are generally determined from MOR bar tests. It is important to note that the MOR is not an intrinsic material parameter but depends on the geometry of the MOR bar and test fixture. A convenient formula for scaling the MOR value from one geometry and test fixture to another is:

$$\frac{MOR_B}{MOR_A} = \left(\frac{b_A h_A}{b_B h_B}\right)^{1/m} \left(\frac{L_{A1} + mL_{A2}}{L_{B1}+mL_{B2}}\right)^{1/m} \qquad (13)$$

The subscripts here identify bar and fixture A and bar and fixture B. This formula assumes four-point loading with the inner span place symmetrically with respect to the outer span. This formula was used to scale the MOR values furnished by AMMRC to standard "A-size" MOR values. The Weibull equation has been shown to be very effective for predicting the experimental failure distributions of complex structure from data bases obtained on MOR bar tests[8], [10].

4. FINITE ELEMENT MODEL

The finite element model set up to simulate the hub is shown in Fig. 2. It has 216 elements and 243 nodes. The elements and nodes are numbered horizontally from right to left, starting at the bore. Element numbers are located in the center of the element, and node numbers are shown on the exterior of the grid. Node numbers 236, 237, 238, 240, 241, and 242 were located with respect to the centerline to coincide with the location of the forces used to simulate the blade loads. Not all node and element numbers are shown on the mesh in Fig. 2., but any one may be located by counting horizontally. The node and element numbers are needed for interpreting the forces used to simulate blade loads and the heat transfer data.

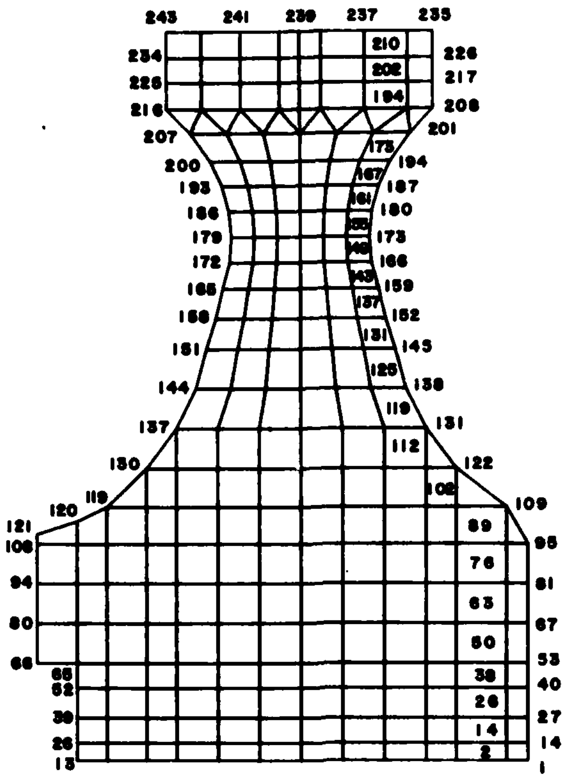

Fig. 2. Disk finite element grid.

5. MATERIAL DATA

The calculation of temperatures, stresses, fast fracture and time dependent reliabilities requires a number of material properties. These properties were supplied by AMMRC or it was suggested that a particular property was similar to the property of a known material. The properties used are given in the Appendix B. AMMRC suggested that the thermal properties of Norton's NC-132 be used and thus the thermal properties given in Table I are for NC-132.

The elastic properties are given in Table II. Young's modulus, Poisson's ratio, and shear modulus were furnished in graphical form and are reproduced here in tabular form. The coefficient of thermal expansion was furnished in tabular form, Table II.

AMMRC furnished modulus of rupture data, giving the values for 50% probability of failure; however, the size of the MOR bar was not that of a standard "A" size bar. This required two conversions to get the MOR bar data into the values accepted by Ford's codes for calculating fast fracture reliability. First the characteristic MOR was calculated from Eqn. 14

$$P_f = 1 - \exp - \frac{(MOR\ )^m}{MOR_o} \tag{14}$$

where P_f = 0.5, MOR = the value furnished for 50% probability of failure, and m=15. The results were then scaled to the standard "A" size bar using Eqn. 13, which with the bar dimensions and the given Weibull modulus of 15 becomes

$$\frac{MOR_B}{MOR_A} = 1.0367 \tag{15}$$

The results after these two conversions are presented in Table III.

The time dependent material properties are given in Table IV. The values were furnished for 1100, 1150, 1200, and 1250°C. Most of the computed tempertures in the disc were below 1100°C, with temperatures down to 787°C. Since values of B and n are required at all temperatures the B and n values furnished for 1100°C were assumed to apply down to room temperature. The alternate approach in the absence of values for B and n is to use a lower limit on temperature below which no crack growth is assumed to occur. This approach was not used in this report, since a lower limit was not furnished. The value of B furnished was assumed to be the one obtained from the application of Eqn. 7.

6. MECHANICAL STRESSES

The primary purpose of this report is to calculate time dependent reliabilities and the associated temperatures and stresses; however, for interpreting the results it is useful to have the stresses due to centrifugal effects. This section presents these stresses at room temperature. Table V shows the forces used to simulate blade loads and the node number at which the particular load was applied. This data was furnished in tabular form by AMMRC. The mesh was constructed so that the nodes were locted to correspond with the geometric location. The forces were applied radially outward at these nodes.

The rotational speed at which the stresses were calculated was 61,500 rpm. The maximum principal stresses are plotted in Fig. 3. The bore stress is 165 MPa, and the neck stress is 125 MPa. The tangential and radial stresses are plotted in Figs. 4 and 5 respectively. The isostress plots are in increments of 5 MPa. The fast fracture probability of failure for these stresses and the Weibull data given in Table III is 3.725×10^{-8}.

7. COMBINED THERMAL AND MECHANICAL STRESSES

This section presents the results of the analysis of the combined thermal and mechanical stresses. In the analysis a steady state temperature distribution and no creep was assumed. The heat transfer data furnished was in graphical form. In order to input the data into the computer code it was necessary to convert the data into numerical

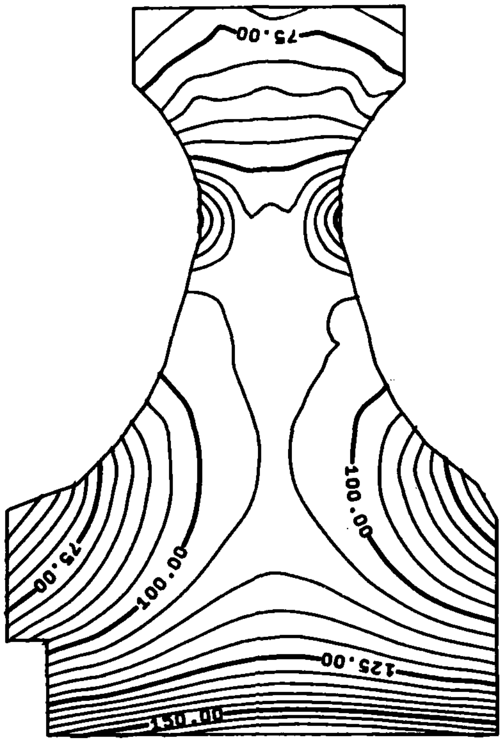

Fig. 3. Maximum principal stresses [MPa]
in disc, centrifugal stresses.

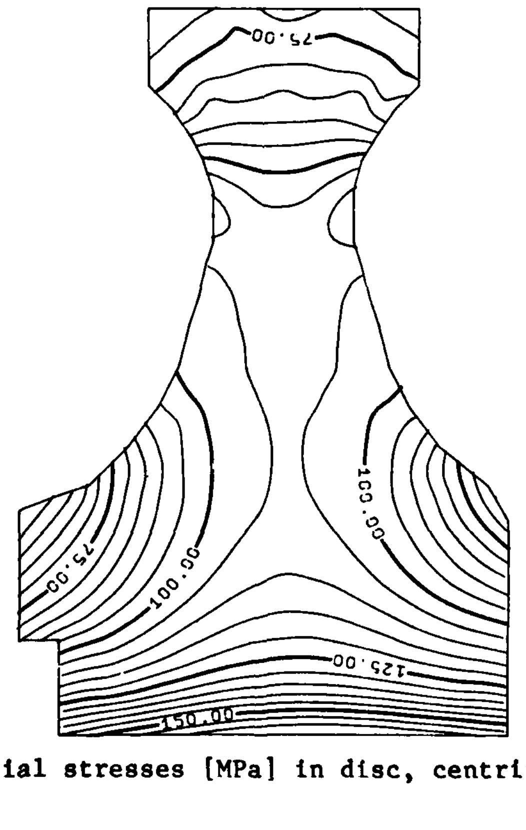

Fig. 4. Tangential stresses [MPa] in disc, centrifugal stresses.

form. Table VI gives the data as prepared for the computer. Shown are the heat transfer coefficients and adiabatic wall temperatures and the corresponding element and node numbers. Data was supplied for the pedestal, and upstream and downstream faces of the disc. The data furnished assumed no heat transfer in the bore and at the attachments; therefore, all surfaces not listed in Table VI were treated as being adiabatic. The steady state temperatures calculated from these boundry conditions are plotted in Fig. 6. Temperatures shown are in degrees centigrade, and the maximum calculated nodal temperature is 1121°C at node 216.

The combined stresses due to the thermal gradients shown in Fig. 6 and the centrifugal loads given in the previous section were calculated and were plotted in Figs. 7, 8, and 9. These are the maximum principal, tangential, and radial stresses, respectively. The maximum bore stress is 220 MPa and the maximum stress in the neck is 200 MPa. The gradient between the isostress lines is 5 MPa.

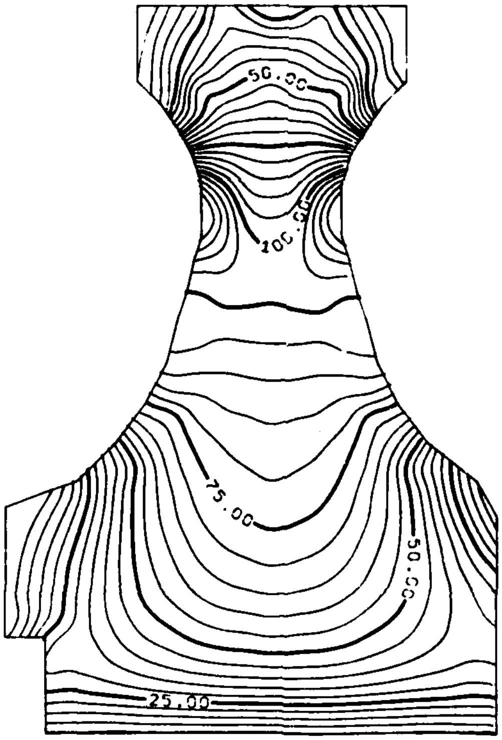

Fig. 5. Radial stresses [MPa] in disc, centrifugal stresses

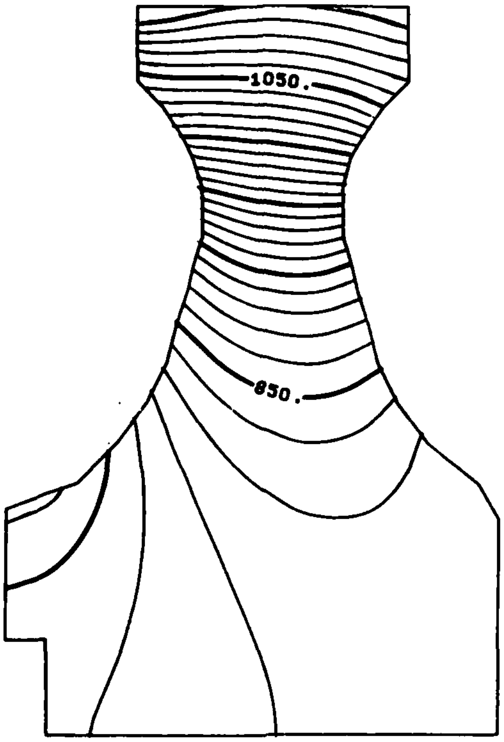

Fig. 6. Isotherms [°C] in disc of 61500 rpm.

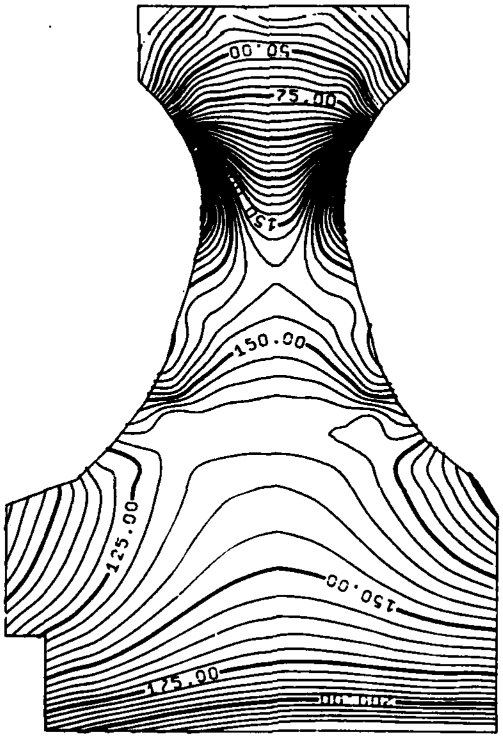

Fig. 7. Maximum principal stresses [MPa] in disc, combining thermal and centrifugal stresses at 61500 rpm.

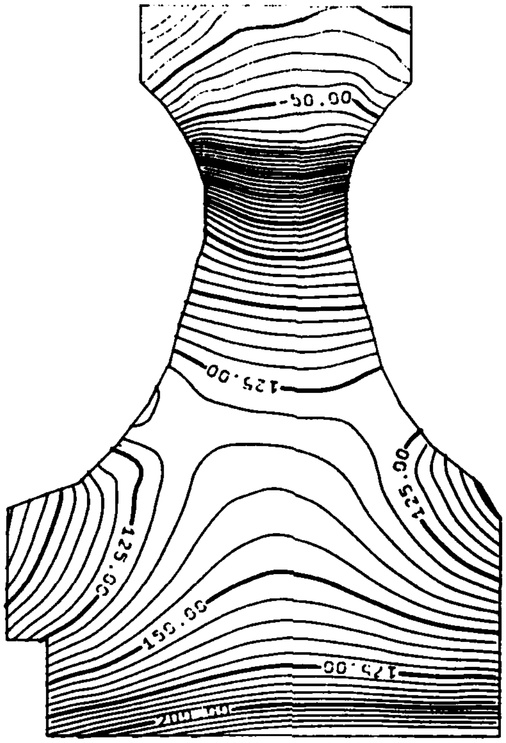

Fig. 8. Tangential stresses [MPa] in disc combining thermal and centrifugal stresses at 61500 rpm.

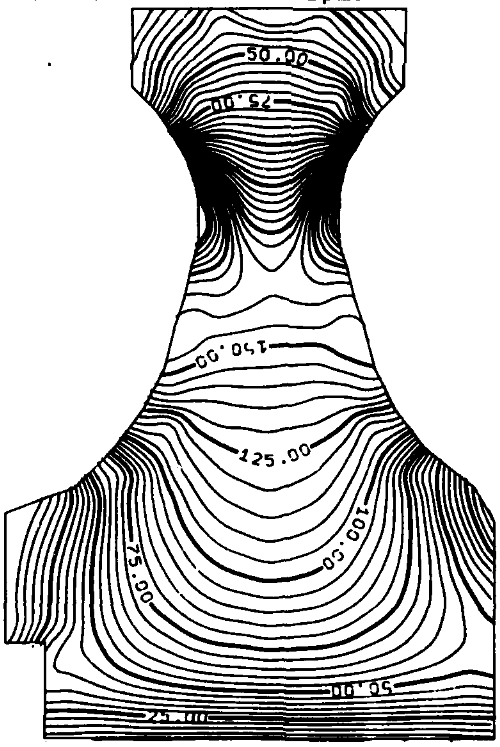

Fig. 9. Radial stesses [MPa] in disc, combining thermal and centrigual stresses at 61500 rpm.

8. RELIABILITIES

The reliability versus time for the disc was calculated for up to 1000 hours of steady state running and the result is plotted in Fig. 10. The fast fracture reliability, that is the reliability at time equal zero, is 0.99982. The time dependent parameters used are in Table IV. The results assume continuous opertion at 61500 rpm at the temperatures shown in Fig. 6. The effects of creep and oxidation are assumed to be negligible. The maximum principal stress in the bore 225 MPa at a temperature of 823°C. The reliability for steady state running at these conditions is at time equal zero, 0.99982, and at time equal 1000 hours, 0.667.

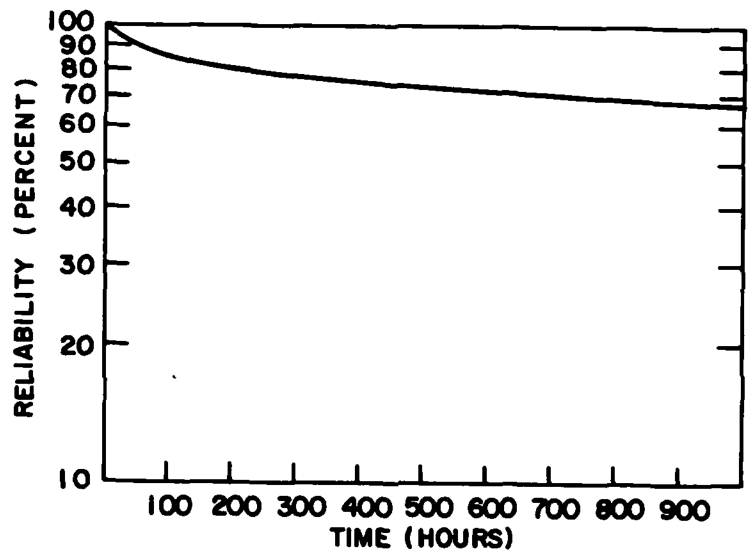

Fig. 10. Reliability versus time for steady state operation.

9. SUMMARY

The mechanical stresses and combined mechanical and thermal stresses were calculated for a hot pressed silicon nitride turbine disc. At room temperature the maximum principal stress was 165 MPa due to mechanical loads at 61500 rpm. The corresponding fast fracture probability of failure was 3.725×10^{-8}. The steady state temperature distribution was calculated for the boundary conditions at 61500 rpm. The maximum temperature in the bore was 824°C, the maximum temperature in the neck was 946°C, and the maximum temperature on the platform was 1121°C. The thermal stresses due to this temperature distribution were combined with the stresses due to mechanical loads at elevated temperatures. At these conditions the maximum principal stress in the bore was 225 MPa at 823°C, and the maximum principal stress in the neck was 210 MPa at 929°C.

The reliabilities versus time were calculated, assuming no creep and continuous running at 61500 rpm, for the combined stress and steady state temperature conditions. At time equal to zero the calculated reliability is 0.99982 and at 1000 hours the reliability is 0.667.

10. REFERENCES

1. Siverns, M. J. and Price, A. T., "Crack Growth Under Creep Conditions." Nature, November 21, 1970.

2. Siverns, M. J. and Price, A. J., "Crack Propagation Under Creep Conditions in a Quenched 2-1/4 Chromium 1 Molybdenum Steel." International Journal of Fracture, June, 1973.

3. Evans, A. G., and Widerhorn, S. M., "Proof Testing of Ceramic Materials and Analytical Basis for Failure Prediction." International Journal of Fracture, September, 1974.

4. Evans, A. G., "Understanding the Characteristics of Brittle Materials." ASME Paper 75-GT-87.

5. Paluszny, A. and Nicholls, P. F., "Predicting Time-Dependent Reliability of Ceramic Rotors." Ceramics for High Performance Applictions-II. Eds. John J. Burke, Edward N. Lenoe, and R. Nathan Katz, Chestnut Hill, Massachusetts, Brook Hill, 1978.

6. Weibull, W., "A Statistical Theory of the Strength of Materials," Proceedings of the Royal Swedish Institute for Engineering Research, Stockholm, 1939.

7. Baker, R. R., Swank, L. R., and Caverly, J. C., "Ceramic Life Prediction Methodology - Hot Spin Disc Life Program Interim Report." AMMRC TR 82-26, April, 1982.

8. Vardar, O. and Finnie, I., "An Analysis of the Brazilian Disc Fracture Test Using the Weibull Probabilistic Treatment of Brittle Strength." International Journal of Fracture, June, 1979.

9. Manson, S. S., Thermal stress and Low - Cycle Fatigue, McGraw-Hill, New York, 1966.

10. Swank, L. R. and Williams, R. M., "Correlation of Static Strengths and Speeds of Rotational Failure of Structural Ceramics," American Ceramic Society Bulletin, August, 1981.

11. APPENDIX A NOMENCLATURE

a Crack length, m

a_o Initial crack length, m

A Area on unit sphere, m^2

A Premultiplier in crack velocity equation, meter/second $(MPa\text{-}m)^n$

B Constant in reliability versus time equation, MPa^2-hr

B Risk of rupture

b Width of MOR specimen, m

h Height of MOR specimen, m

K Constant, defined by Eqn. 10

K_I Stress intensity $MPa\sqrt{m}$

K_{IC} Critical stress intensity, a material parameter, $MPa\sqrt{m}$

L_1 Bottom span of MOR specimen, m

L_2 Top span of MOR specimen, m

m Weibull Modulus

MOR Modulus of rupture, MPa

MOR_o Characteristic modulus of rupture, MPa

n Crack velocity exponent

P_f Probability of failure

R Reliability as a function of time

R_{ff} Fast fracture reliability

σ Stress, MPa

σ_θ Characteristic strength of the structure, MPa

σ_n Normal stress, MPa

$\sigma_1, \sigma_2, \sigma_3$ Maximum principal stresses, MPa

σ_o Weibull parameter, $MPa/(m^3)^{1/m}$

t	Time, hours
V	Volume, m^3
V	Crack velocity, m/sec
Y	Stress intensity factor coefficient, non-dimensional
ψ	Azimuthal angle
ϕ	Polar angle

TABLE I

Thermal Properties

	Temperature °C	Thermal Conductivity $\frac{\text{watt}}{\text{meter °C}}$	Specific Heat $\frac{\text{joule}}{\text{kg °C}}$
Hot Pressed Silicon	21.	29.4	754.
Nitride	260.	26.0	963.
Density = 3.19 gm/cm^3	538.	22.5	1088.
	816.	19.0	1214.
	1092.	15.9	1381.
	1371.	13.8	1340.

TABLE II

Elastic Properties

	Temp.	Young's Modulus	Poisson's Ratio	Shear Modulus	Coefficient of Thermal Expansion
Hot Pressed Silicon Nitride	°C	GN/m^2		GN/m^2	1/°C
Density =3.19 gm/cm^3	23.	320.	.280	122.	1.13
	600.	311.	.278	121.	3.39
	800.	308.	.277	120.	3.59
	1000.	301.	.275	118.	3.67
	1100.	297.	.274	116.	3.47
	1200.	287.	.276	112.	3.45
	1300.	274.	.276	108.	3.43
	1400.	257.	.274	101.	3.25

TABLE III

Fast Fracture Properties

Temperature °C	Characteristic MOR MPa	Weibull Modulus
20	733.	15.
900	568.	15.
1000	532.	15.
1100	480.	15.
1200	425.	15.
1250	373.	15.

Specimen Dimensions ("A"-size bar)

Width	6.350 mm
Height	3.175 mm
Inner span	9.525 mm
Outer span	19.050 mm

TABLE IV

Time Dependent Properties

Temperature °C	Parameter B MPa^2-Sec	Crack Velocity Exponent
21	515.	40
1100	515.	40
1150	515.	40
1200	8.81	40
1250	.12	40

TABLE V

Forces Simulating Blade Loads

Node Number	Force Newtons
236	5148.8
237	12821.9
238	15903.6
240	15996.9
241	13617.0
242	5631.7

TABLE VI

Heat Transfer Data

	Element Number	Node 1	Node 2	Heat Transfer Coefficient $\frac{W}{m^2 \, °K}$	Adiabatic Wall Temperature °C
Pedestal	216	243	242	2650.	1250
	215	242	241	1480.	1250
	214	241	240	1260.	1250
	213	240	239	1230.	1250
	212	239	238	1200.	1250
	211	238	237	1180.	1250
	210	237	236	1150.	1250
	209	236	235	1130.	1250
Upstream	100	121	120	1170.	700
Face of Disc	99	120	119	1150.	701
	110	119	130	1090.	709
	118	130	137	1030.	712
	124	137	144	970.	722
	130	144	151	925.	730
	136	151	158	885.	737
	142	158	165	850.	745
	148	165	172	815.	750
	154	172	179	790.	757
	160	179	186	760.	763
	166	186	193	730.	772
	172	193	200	710.	776
	178	200	207	690.	795
	192	207	216	660.	820
	200	216	225	640.	900
	208	225	234	625.	1042
	216	234	243	608.	1150
Downstream	88	95	109	580.	755
Face of Disc	101	109	122	550.	757
	111	122	131	520.	763
	119	131	138	490.	776
	125	138	145	465.	786
	131	145	152	450.	795
	137	152	159	435.	800
	143	159	166	420.	810
	149	166	173	410.	815
	155	173	180	400.	825
	161	180	187	390.	835
	167	187	194	383.	845
	173	194	201	380.	900
	179	201	208	370.	995
	193	208	217	365.	1100
	201	217	226	355.	1230
	209	226	235	350.	1305

DISTRIBUTION LIST

No. of Copies	To
	Office of the Under Secretary of Defense for Research and Engineering, The Pentagon, Washington, DC 20301
1	ATTN: Mr. J. Persh
1	Dr. G. Gamota
12	Commander, Defense Technical Information Center, Cameron Station, Building 5, 5010 Duke Street, Alexandria, VA 22314
1	National Technical Information Service, 5285 Port Royal Road, Springfield, VA 22161
	Director, Defense Advanced Research Projects Agency, 1400 Wilson Boulevard, Arlington, VA 22209
1	ATTN: Dr. A. Bement
1	Dr. Van Reuth
1	MAJ Harry Winsor
	Battelle Columbus Laboratories, Metals and Ceramics Information Center, 505 King Avenue, Columbus, OH 43201
1	ATTN: Mr. Winston Duckworth
1	Dr. D. Niesz
1	Dr. R. Wills
	Deputy Chief of Staff, Research, Development, and Acquisition, Headquarters, Department of the Army, Washington, DC 20301
1	ATTN: DAMA-ARZ
1	DAMA-CSS, Dr. J. Bryant
	Commander, U.S. Army Medical Research and Development Command, Fort Detrick, Frederick, MD 21701
1	ATTN: SGRD-SI, Mr. Lawrence L. Ware, Jr.
	Commander, Army Research Office, P.O. Box 12211, Research Triangle Park, NC 27709
1	ATTN: Information Processing Office
1	Dr. G. Mayer
1	Dr. J. Hurt
	Commander, U.S. Army Materiel Development and Readiness Command, 5001 Eisenhower Avenue, Alexandria, VA 22333
1	ATTN: DRCDMD-ST
1	DRCLDC
	Commander, Harry Diamond Laboratories, 2800 Powder Mill Road, Adelphi, MD 20783
1	ATTN: Mr. A. Benderly
1	Technical Information Office
1	DELHD-RAE
	Commander, U.S. Army Missile Command, Redstone Arsenal, AL 35809
1	ATTN: Mr. P. Ormsby
1	Technical Library
	Commander, U.S. Army Aviation Research and Development Command, 4300 Goodfellow Boulevard, St. Louis, MO 63120
1	ATTN: DRDAV-EGX
1	DRDAV-QE
	Commander, U.S. Army Tank-Automotive Command, Warren, MI 48090
1	ATTN: Dr. W. Bryzik
1	Mr. E. Hamperian
1	D. Rose
1	DRSTA-RKA
1	DRSTA-UL, Technical Library
1	DRSTA-R
	Commander, U.S. Army Armament Research and Development Command, Dover, NJ 07801
1	ATTN: Dr. G. Vezzoli
1	Technical Library
	Commander, U.S. Army Armament Materiel Readiness Command, Rock Island, IL 61299
1	ATTN: Technical Library
	Commander, Aberdeen Proving Ground, MD 21005
1	ATTN: DRDAR-CLB-PS, Mr. J. Vervier
	Commander, U.S. Army Mobility Equipment Research and Development Command, Fort Belvoir, VA 22060
1	ATTN: DRDME-EM, Mr. W. McGovern
1	DRDME-V, Mr. E. York
	Director, U.S. Army Ballistic Research Laboratory, Aberdeen Proving Ground, MD 21005
1	ATTN: DRDAR-TSB-S (STINFO)
	Commander, U.S. Army Test and Evaluation Command, Aberdeen Proving Ground, MD 21005
1	ATTN: DRSTE-ME
	Commander, U.S. Army Foreign Science and Technology Center, 220 7th Street, N.E., Charlottesville, VA 22901
1	ATTN: Military Tech, Mr. W. Marley
	Commander, Watervliet Arsenal, Watervliet, NY 12189
1	ATTN: Dr. T. Davidson
	Director, Eustis Directorate, U.S. Army Mobility Research and Development Laboratory, Fort Eustis, VA 23604
1	ATTN: Mr. J. Robinson, DAVDL-E-MOS (AVRADCOM)
1	Mr. C. Walker
	Chief of Naval Research, Arlington, VA 22217
1	ATTN: Code 471
1	Dr. A. Diness
1	Dr. R. Pohanka
	Naval Research Laboratory, Washington, DC 20375
1	ATTN: Dr. J. M. Krafft - Code 5830
1	Mr. R. Rice
	Headquarters, Naval Air Systems Command, Washington, DC 20360
1	ATTN: Code 5203
1	Code MAT-042M
1	Mr. I. Macklin
	Commander, Naval Weapons Center, China Lake, CA 93555
1	ATTN: Mr. F. Markarian
	Commander, U.S. Air Force of Scientific Research, Building 410, Bolling Air Force Base, Washington, DC 20332
1	ATTN: MAJ W. Simmons
	Commander, U.S. Air Force Wright Aeronautical Laboratories, Wright-Patterson Air Force Base, OH 45433
1	ATTN: AFWAL/MLLM, Dr. N. Tallan
1	AFWAL/MLLM, Dr. H. Graham
1	AFWAL/MLLM, Dr. R. Ruh
1	AFWAL/MLLM, Dr. A. Katz
1	AFWAL/MLLM, Mr. K. S. Mazdiyasni
1	Aero Propulsion Labs, Mr. R. Marsh
	National Aeronautics and Space Administration, Washington, DC 20546
1	ATTN: Mr. G. C. Deutsch - Code RW
1	Mr. J. Gangler
1	AFSS-AD, Office of Scientific and Technical Information
	National Aeronautics and Space Administration, Lewis Research Center, 21000 Brookpark Road, Cleveland, OH 44135
1	ATTN: J. Accurio, USAMRDL
1	Dr. H. B. Probst, MS 49-1
1	Dr. R. Ashbrook
1	Dr. S. Dutta
1	Mr. S. Grisaffe
	National Aeronautics and Space Administration, Langley Research Center, Center, Hampton, VA 23665
1	ATTN: Mr. J. Buckley, Mail Stop 387
	Department of Energy, Division of Transportation, 20 Massachusetts Avenue, N.W., Washington, DC 20545
1	ATTN: Mr. George Thur (TEC)
1	Mr. Robert Schulz (TEC)
1	Mr. John Neal (CLNRT)
1	Mr. Steve Wander (Fossil Fuels)
	Department of Transportation, 400 Seventh Street, S.W., Washington, DC 20590
1	ATTN: Mr. M. Lauriente
	National Bureau of Standards, Washington, DC 20234
1	ATTN: Dr. S. Wiederhorn
	National Research Council, National Materials Advisory Board, 2101 Constitution Avenue, Washington, DC 20418
1	ATTN: D. Groves
1	R. M. Spriggs
	National Science Foundation, Washington, DC 20550
1	ATTN: B. A. Wilcox

No. of Copies	To
	Admiralty Materials Technology Establishment, Polle, Dorset BH16 6JU, UK
1	ATTN: Dr. D. Godfrey
1	Dr. M. Lindley
	AiResearch Manufacturing Company, AiResearch Casting Company, 2525 West 190th Street, Torrance, CA 90505
1	ATTN: Mr. K. Styhr
	AiResearch Manufacturing Company, Materials Engineering Dept., 111 South 34th Street, P.O. Box 5217, Phoenix, AZ 85010
1	ATTN: Mr. D. W. Richerson, MS 93-393/503-44
	AVCO Corporation, Applied Technology Division, Lowell Industrial Park, Lowell, MA 01887
1	ATTN: Dr. T. Vasilos
	Carborundum Company, Research and Development Division, P.O. Box 1054, Niagara Falls, NY 14302
1	ATTN: Dr. J. A. Coppola
	Case Western Reserve University, Department of Metallurgy, Cleveland, OH 44106
1	ATTN: Prof. A. H. Heuer
	Cummins Engine Company, Columbus, IN 47201
1	ATTN: Mr. R. Kamo
	Deposits and Composites, Inc., 1821 Michael Faraday Drive, Reston, VA 22090
1	ATTN: Mr. R. E. Engdahl
	Electric Power Research Institute, P.O. Box 10412, 3412 Hillview Avenue, Palo Alto, CA 94304
1	ATTN: Dr. A. Cohn
	European Research Office, 223 Old Maryleborne Road, London, NW1 - 5the, England
1	ATTN: Dr. R. Quattrone
1	LT COL James Kennedy
	Ford Motor Company, Turbine Research Department, 20000 Rotunda Drive, Dearborn, MI 48121
1	ATTN: Mr. A. F. McLean
1	Mr. E. A. Fisher
1	Mr. J. A. Mangels
1	Mr. R. Govila
	General Electric Company, Research and Development Center, Box 8, Schenectady, NY 12345
1	ATTN: Dr. R. J. Charles
1	Dr. C. D. Greskovich
1	Dr. S. Prochazka
	General Motors Corporation, AC Spark Plug Division, Flint, MI 48556
1	ATTN: Dr. M. Berg
	Georgia Institute of Technology, EES, Atlanta, GA 30332
1	ATTN: Mr. J. D. Walton
	GTE Laboratories, Waltham Research Center, 40 Sylvan Road, Waltham, MA 02154
1	ATTN: Dr. C. Quackenbush
1	Dr. W. H. Rhodes
	IIT Research Institute, 10 West 35th Street, Chicago, IL 60616
1	ATTN: Mr. S. Bortz, Director, Ceramics Research
	Institut fur Werkstoff-Forschung, DFVLR, 505 Porz-Wahn, Linder Hohe, Germany
1	ATTN: Dr. W. Bunk
	International Harvester, Solar Division, 2200 Pacific Highway, P.O. Box 80966, San Diego, CA 92138
1	ATTN: Dr. A. Metcalfe
1	Ms. M. E. Gulden

No. of Copies	To
	Kawecki Berylco Industries, Inc., P.O. Box 1462, Reading, PA 19603
1	ATTN: Mr. R. J. Longenecker
	Martin Marietta Laboratories, 1450 South Rolling Road, Baltimore, MD 21227
1	ATTN: Dr. J. Venables
	Massachusetts Institute of Technology, Department of Metallurgy and Materials Science, Cambridge, MA 02139
1	ATTN: Prof. R. L. Coble
1	Prof. H. K. Bowen
1	Prof. W. D. Kingery
	Midwest Research Institute, 425 Volker Boulevard, Kansas City, MO 64110
1	ATTN: Mr. Gordon W. Gross, Head, Physics Station
	Norton Company, Worcester, MA 01606
1	ATTN: Dr. N. Ault
1	Dr. M. L. Torti
	Pennsylvania State University, Materials Research Laboratory, Materials Science Department, University Park, PA 16802
1	ATTN: Prof. R. E. Tressler
1	Prof. R. Bradt
1	Prof. V. S. Stubican
	RIAS, Division of the Martin Company, Baltimore, MD 21203
1	ATTN: Dr. A. R. C. Westwood
	Stanford Research International, 333 Ravenswood Avenue, Menlo Park, CA 94025
1	ATTN: Dr. P. Jorgensen
1	Dr. D. Rowcliffe
	State University of New York at Stony Brook, Department of Materials Science, Long Island, NY 11790
1	ATTN: Prof. Franklin F. Y. Wang
	United Technologies Research Center, East Hartford, CT 06108
1	ATTN: Dr. J. Brennan
1	Dr. F. Galasso
	University of California, Lawrence Livermore Laboratory, P.O. Box 808, Livermore, CA 94550
1	ATTN: Dr. C. F. Cline
	University of Florida, Department of Materials Science and Engineering, Gainesville, FL 32601
1	ATTN: Dr. L. Hench
	University of Newcastle Upon Tyne, Department of Metallurgy and Engineering Materials, Newcastle Upon Tyne, NEI 7 RU, England
1	ATTN: Prof. K. H. Jack
	University of Washington, Ceramic Engineering Division, FB-10, Seattle, WA 98195
1	ATTN: Prof. James I. Mueller
	Westinghouse Electric Corporation, Research Laboratories, Pittsburgh, PA 15235
1	ATTN: Dr. R. J. Bratton
	Director, Army Materials and Mechanics Research Center, Watertown, MA 02172
2	ATTN: DRXMR-PL
1	DRXMR-PR
1	DRXMR-K
1	DRXMR-FD
10	DRXMR-SM, Dr. E. Lenoe

Army Materials and Mechanics Research Center
Watertown, Massachusetts 02172
Ceramic Life Prediction Methodology-
Analytical Assessment of Selected
Component Data
L. R. Swank

AD ____________
UNCLASSIFIED
UNLIMITED DISTRIBUTION

Technical Report AMMRC TR 82-50, September 1982,
24 pp- illus-tables, Contract DAAG 46-77-C-0028

Key Words
Brittle design
Ceramics
High temperature materials
Silicon nitride

A complete set of thermal conditions, mechanical loads, geometry as well as thermal, elastic, fast fracture, and time dependent material properties was furnished by AMMRC for the hub of a gas turbine disc. A finite element computer model was prepared for the disc from this data. The temperture and stress distributions, the fast fracture and the time dependent reliabilities were calculated. The results were presented in iso-stress and iso-thermal plots and in graphical data.

Army Materials and Mechanics Research Center
Watertown, Massachusetts 02172
Ceramic Life Prediction Methodology-
Analytical Assessment of Selected
Component Data
L. R. Swank

AD ____________
UNCLASSIFIED
UNLIMITED DISTRIBUTION

Technical Report AMMRC TR 82-50, September 1982,
24 pp- illus-tables, Contract DAAG 46-77-C-0028

Key Words
Brittle design
Ceramics
High temperature materials
Silicon nitride

A complete set of thermal conditions, mechanical loads, geometry as well as thermal, elastic, fast fracture, and time dependent material properties was furnished by AMMRC for the hub of a gas turbine disc. A finite element computer model was prepared for the disc from this data. The temperture and stress distributions, the fast fracture and the time dependent reliabilities were calculated. The results were presented in iso-stress and iso-thermal plots and in graphical data.

Army Materials and Mechanics Research Center
Watertown, Massachusetts 02172
Ceramic Life Prediction Methodology-
Analytical Assessment of Selected
Component Data
L. R. Swank

AD ____________
UNCLASSIFIED
UNLIMITED DISTRIBUTION

Technical Report AMMRC TR 82-50, September 1982,
24 pp- illus-tables, Contract DAAG 46-77-C-0028

Key Words
Brittle design
Ceramics
High temperature materials
Silicon nitride

A complete set of thermal conditions, mechanical loads, geometry as well as thermal, elastic, fast fracture, and time dependent material properties was furnished by AMMRC for the hub of a gas turbine disc. A finite element computer model was prepared for the disc from this data. The temperture and stress distributions, the fast fracture and the time dependent reliabilities were calculated. The results were presented in iso-stress and iso-thermal plots and in graphical data.

Army Materials and Mechanics Research Center
Watertown, Massachusetts 02172
Ceramic Life Prediction Methodology-
Analytical Assessment of Selected
Component Data
L. R. Swank

AD ____________
UNCLASSIFIED
UNLIMITED DISTRIBUTION

Technical Report AMMRC TR 82-50, September 1982,
24 pp- illus-tables, Contract DAAG 46-77-C-0028

Key Words
Brittle design
Ceramics
High temperature materials
Silicon nitride

A complete set of thermal conditions, mechanical loads, geometry as well as thermal, elastic, fast fracture, and time dependent material properties was furnished by AMMRC for the hub of a gas turbine disc. A finite element computer model was prepared for the disc from this data. The temperture and stress distributions, the fast fracture and the time dependent reliabilities were calculated. The results were presented in iso-stress and iso-thermal plots and in graphical data.